STEREOMAPPING WITH SPOT-P AND ERS-1 SAR IMAGES

Thierry Toutin
Canada Centre for Remote Sensing
588 Booth Street, Ottawa, Ontario, Canada K1A 0Y7
Tel: (613) 947-1293
Fax: (613) 947-1385
E-mail: thierry.toutin@ccrs.nrcan.gc.ca

ABSTRACT

This paper reports on some aspects of using mixed radar and visible sensors to generate stereo pairs that are suitable for stereo mapping planimetric and elevation features. By choosing compromises to reduce geometric and radiometric disparities, the brain is able to perceive depth and to combine the complementary aspects of the radiometries from a VIR/SAR stereo pair. Quantitative results of mapping and feature extraction from opposite and same-side ERS-SAR and SPOT-P stereo images are presented. In planimetry, accuracy of about 30 m is obtained. Such accuracy is dependent on the stereo pair, the stereo viewability, the image content and the feature definition. In altimetry, 20-m accuracies are obtained for both stereo pairs. The strongest stereo geometry does not explicitly lead to better results. With these mixed SAR/VIR stereo pairs the major contributor to the elevation parallax is the SAR geometry. Finally from the stereo-fusion of these two ERS-SAR/SPOT-P pairs, the radiometry of the SPOT-P images mainly contributes to determine the planimetric features with the quality of its image content, while the geometry of the ERS-SAR image mainly contributes to determine the elevation with its high sensitivity to the terrain relief.

1. INTRODUCTION

A large amount of remote sensing images of our planet are regularly acquired by various remote sensing missions covering a wide variety of sensors. Combining and merging of images acquired in the visible and infrared (VIR) and in the microwave spectrum are largely used in earth resources mapping and monitoring to extract geophysical information. The most common method used to fill this need is the geocoding of the different remote sensing images to a defined cartographic reference system. This task requires exact relationship between image acquisition system and ground reference system, which is achieved through a parametric geometric modelling and the integration of digital elevation models (DEM).

Another method related to photogrammetric work is the stereo fusion and the stereoscopic extraction of 3D cartographic information in such a reference system. Many studies have focused on the use of stereo-mapping using images either from optical sensors or from radar sensors with softcopy workstations. Articles by Heipke (1995) and Grün (1997) are updated references on the state-of-the-art of these methods and the associated softcopy workstations.

Most of the latest experiments put the emphasis on developing stereoscopic methods and systems from one type of sensor, either optical or radar. Few results have been published from combination of optical and radar sensors with the stereoscopic method. When Raggam *et al.* (1994) combined airborne SAR with SPOT-HRV data to extract elevation information, they reported "no meaningful results" in the image matching due to many radiometric disparities (the two paths were perpendicular). They then manually measured 500 corresponding image points, but not in stereoscopic mode, and calculated off-line the three cartographic co-ordinates. They achieved a 60-m standard deviation with a 42-m bias with the largest errors around ±250 m. Since they did not use full stereoscopic capabilities, they also did not extract planimetric features such as road, railroads, etc.

In order to further investigate the feasibility, the usefulness and the potential of the stereo fusion from mixed optical and radar sensors by combining geometric and radiometric properties of both sensors, an experiment was done using satellite data: two panchromatic SPOT images and an ERS-1 SAR image over the Rocky Mountains, Canada. These stereo pairs, combining visible and SAR images, provide a great challenge. At the first attempt, human stereo fusion and perception seem almost impossible. However with training and practice, the human brain can learn and acquire this "non-natural" stereo-capability because depth perception is an active system. This paper then addresses geometric and radiometric singularities between the visible and SAR images, their impact on the stereo fusion, and the ways of overcoming these problems.

Finally, the paper addresses the stereo-mapping of planimetric and altimetric features from the two-mixed sensor stereo-pairs. Using a rigorous photogrammetric solution for the geometric modelling already developed at the Canada Centre for Remote Sensing (CCRS) (Toutin, 1995a) on a digital stereo workstation, the DVP, results and accuracies are presented and analysed as a function of geometric and radiometric parameters related to the sensor, the stereo geometry and the terrain.

2. GEOMETRIC AND RADIOMETRIC SINGULARITIES IN DEPTH PERCEPTION

When using two mixed sensor images, the stereoscopic fusion can provide a virtual three-dimensional model of the terrain surface in the observer's brain. This process of stereo fusion and depth perception is not a passive but an active phenomenon in which the eye/brain is the source of the organising power that creates and gives meaning to our visual environment (Friedhoff and Benzon, 1991). The visual system creates the three-dimensional world we experience from the two-dimensional patterns onto the retinas. Depth perception from VIR stereo imagery reproduces the "naturalness" of our visual system. It is no longer true when combining VIR and SAR imagery. But, perception is a matter of experience and relies on an intimate relationship with "object recognition". Unfortunately, at this point we know little about how the brain identifies objects, so a large portion of "depth perception" is not understood (Friedhoff and Benzon, 1991).

However, in modern psychology it is accepted that depth perception is based upon as many as ten physiological and psychological cues (Okoshi, 1976). With remote sensing images, binocular disparity (for stereoscopy) and shade and shadow (for SAR images) are two of the most

important cues. The brain thus combines these cues with the 2D picture to produce judgements about the relationship of objects in space. Finally this suggests that a-priori knowledge is useful for a better interpretation and understanding of the images: to have a clear idea of what to look for, where to look and how to look (Hoffman, 1990). In addition to the experience, a good understanding of the geometric and radiometric singularities is thus important to better perceive and integrate the information and depth from a VIR/SAR stereo-pair.

2.1 Geometric singularities

To obtain good geometry for a better stereo plotting, the intersection angle should be large in order to increase the stereo exaggeration factor or, equivalently the observed parallax, which is used to determine the terrain elevation. For same sensor stereo pairs, an opposite-side stereo configuration then maximises this intersection angle. In a VIR/SAR stereo pair the intersection angle is the angle between projection lines for the VIR data and the range projection circle for the SAR data (Figure 1). Since the elevation displacements in VIR and SAR images occur in the "opposite directions" the opposite-side VIR/SAR configuration generates a subtractive parallax, while it generates an additive parallax for the same-side VIR/SAR configuration. But the major contribution of the elevation parallax is due to the SAR geometry: an elevation parallax factor of 2.1 for an ERS-1 SAR image versus a maximum elevation parallax factor of 0.6 for a 30° view angle SPOT-HRV image (Guindon and Adair 1992, Toutin, 1995a). Consequently, the contribution to the elevation parallax for the VIR image is of the second order in both stereo configurations.

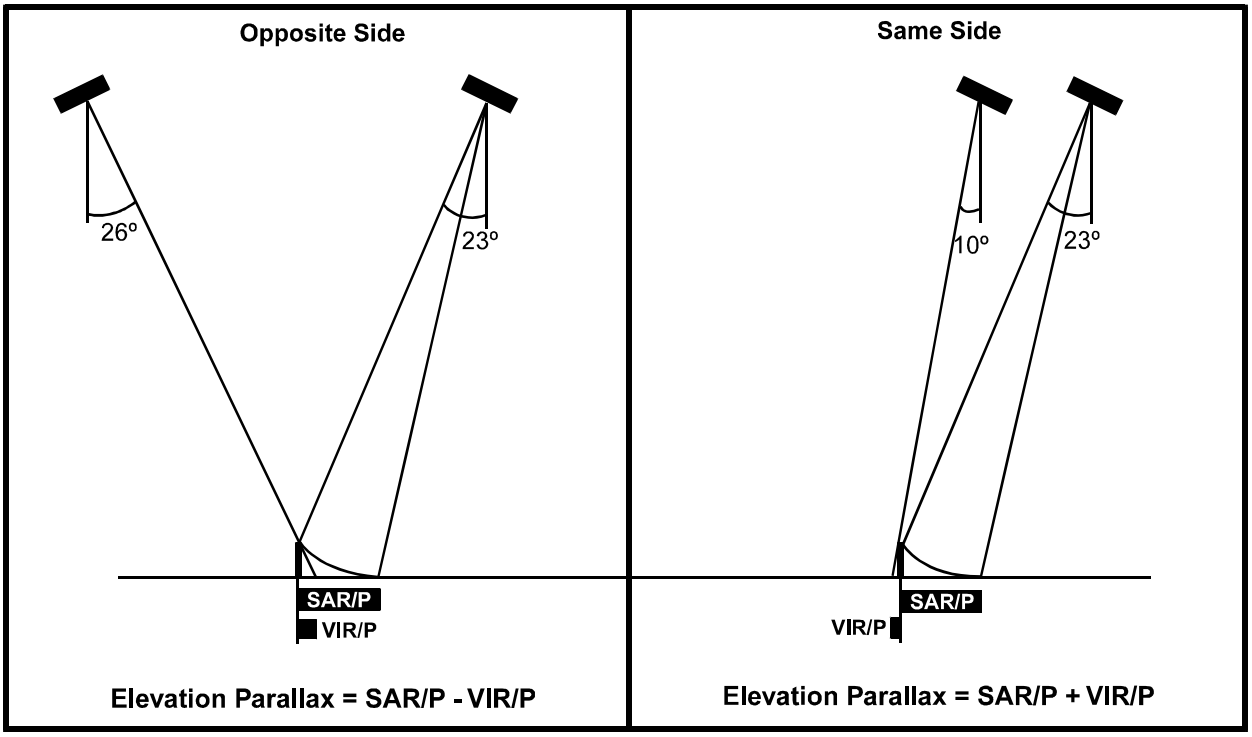

Figure 1: Geometry of a mixed sensor VIR-SAR stereo pairs in opposite and same-side configurations.

To illustrate the different singularities, Figures 2 and 3 (500 pixels by 600 lines) are examples of the opposite and same-side stereo pairs generated with ground range ERS-SAR and panchromatic SPOT-HRV data, respectively. The SPOT data of Figures 2 and 3 were acquired with a viewing angle at the image centres of about +26º and -10º, respectively. More details on the data are given in the next section. The high relief area (800-m elevation variation with up-to-45º slopes) of Figures 2 and 3 have been chosen to display the extreme case of stereo viewing due to relief-induced geometric and radiometric disparities, but also radiometric disparities due to land cover SAR backscatter and VIR reflectance. Only experienced operators can obtain the depth perception over a small area at a time with so many combined geometric and radiometric disparities. Figure 4 (ERS1-SAR/SPOT-HRV11º) is an easier stereo-viewable example due to the moderate relief (200-m elevation variation with 15º maximum slopes), which consequently reduces the geometric and radiometric disparities.

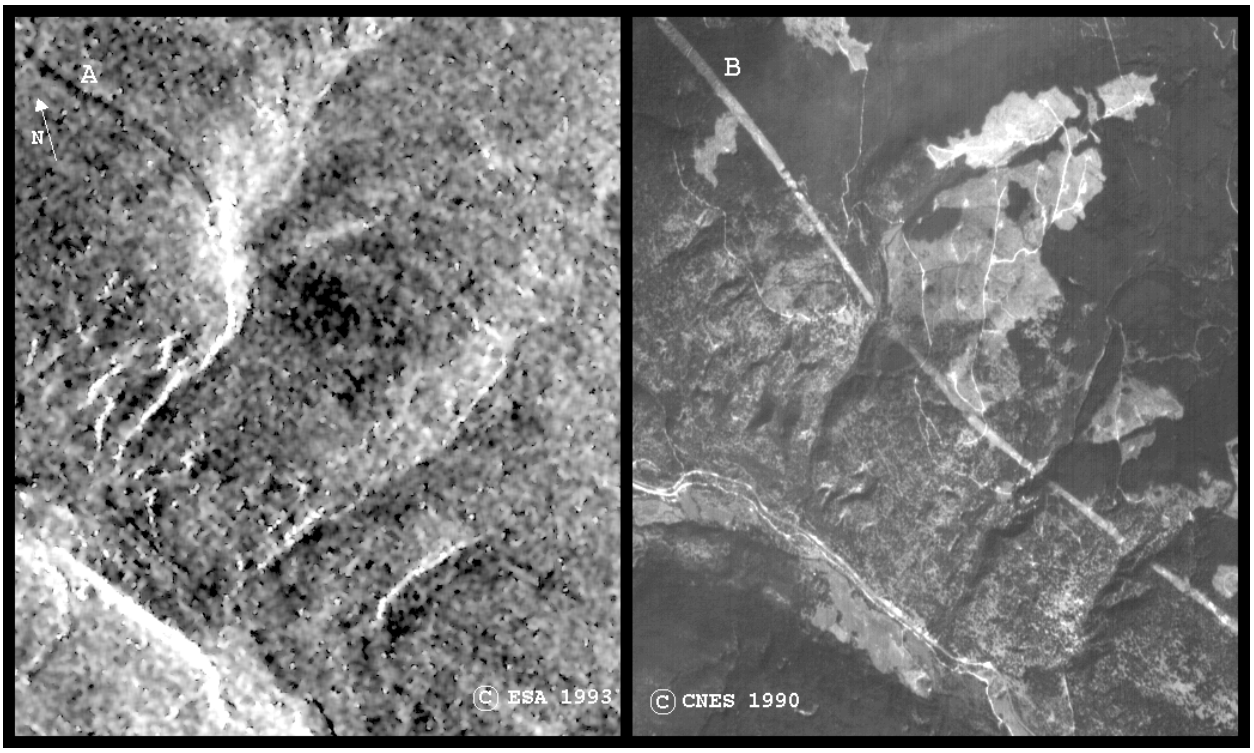

Figure 2: High relief sub-area (800-m elevation and up-to-45° slopes; 500 pixels by 600 lines) of the opposite-side stereo pair ERS-SAR and SPOT-P26 over the Rocky Mountains, Canada. The look direction is westward oriented for the ERS-SAR ground range image (12.5-m pixel spacing) from a descending path, and it is eastward oriented for the SPOT-P26 raw level 1 image (12-m pixel spacing).

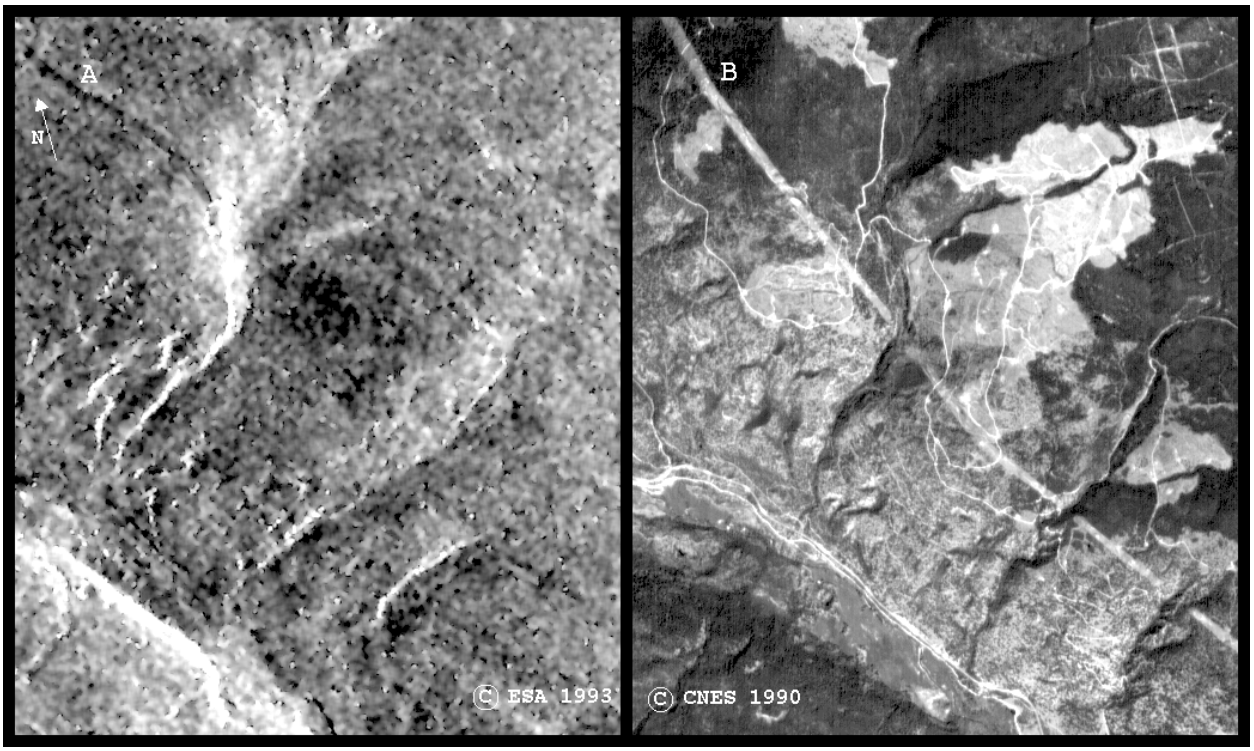

Figure 3: High relief sub-area (800-m elevation and up-to-45° slopes; 500 pixels by 600 lines) of the same-side stereo pair ERS-SAR and SPOT-P10 over the Rocky Mountains, Canada. The look direction is westward oriented for the ERS-SAR ground range image (12.5-m pixel spacing) from a descending path and it is westward for the SPOT-P10 raw level 1 image (11-m pixel spacing).

The resolution of both sensors obviously has an impact on the identification of comparable terrain features between the two images (Figures 2 to 4). However with experience and practice, the stereo-fusion becomes possible: locally (few tens of pixels) for Figures 2 and 3, but more generally (two-third of the stereo pair) for Figure 4. This impact is also addressed in the radiometric disparities. The pixel size (12 m and 11 m for the SPOT-26º and SPOT-11º, respectively) generates some differences in scale, surface and shape of the features. When fusing them in stereo with the ERS-1 SAR image, the 12-m pixel of the SPOT-26º is more consistent with 12.5-m pixel spacing of the ground range ERS-SAR. However, the 11-m pixel of the SPOT-10º does not degrade the stereo viewing and plotting too much by introducing artificial parallaxes. It has been noted during other experiments that a 10% variation in the pixel spacing is acceptable for the stereo-fusion with sensors having approximately the same resolution.

Since the three images were acquired from descending orbits, the small variations in the general orientation of the images do not hinder globally their stereo viewing. Using an ERS-SAR image from an ascending orbit would have generated more singularities and have reduced the stereo viewing to a smaller area at a time. But, there is local change in orientation for some linear features, such as the power line clear-cut ("A" in Figures 2 and 3). It is due to the 800-m mountain elevation which generates a parallax in opposite directions between the two SPOT images (e.g., approximately westward in Figure 2 and eastward Figure 3). As mentioned earlier,

the elevation parallax in the westward direction is also more pronounced for the ERS-SAR image ("B" in Figures 2 and 3). As shown in Figure 1, this example illustrates the subtractive or additive parallaxes for the opposite-side (Figure 2) or same-side (Figure 3) stereo configurations respectively, but also the contribution of the different images to the elevation parallax. The major impact is that the stereo viewing in this area is then more reduced locally with the images of Figure 3 than with the images of Figure 2. Even in some extreme situation, the stereo viewing is reduced at the floating mark level (few pixels).

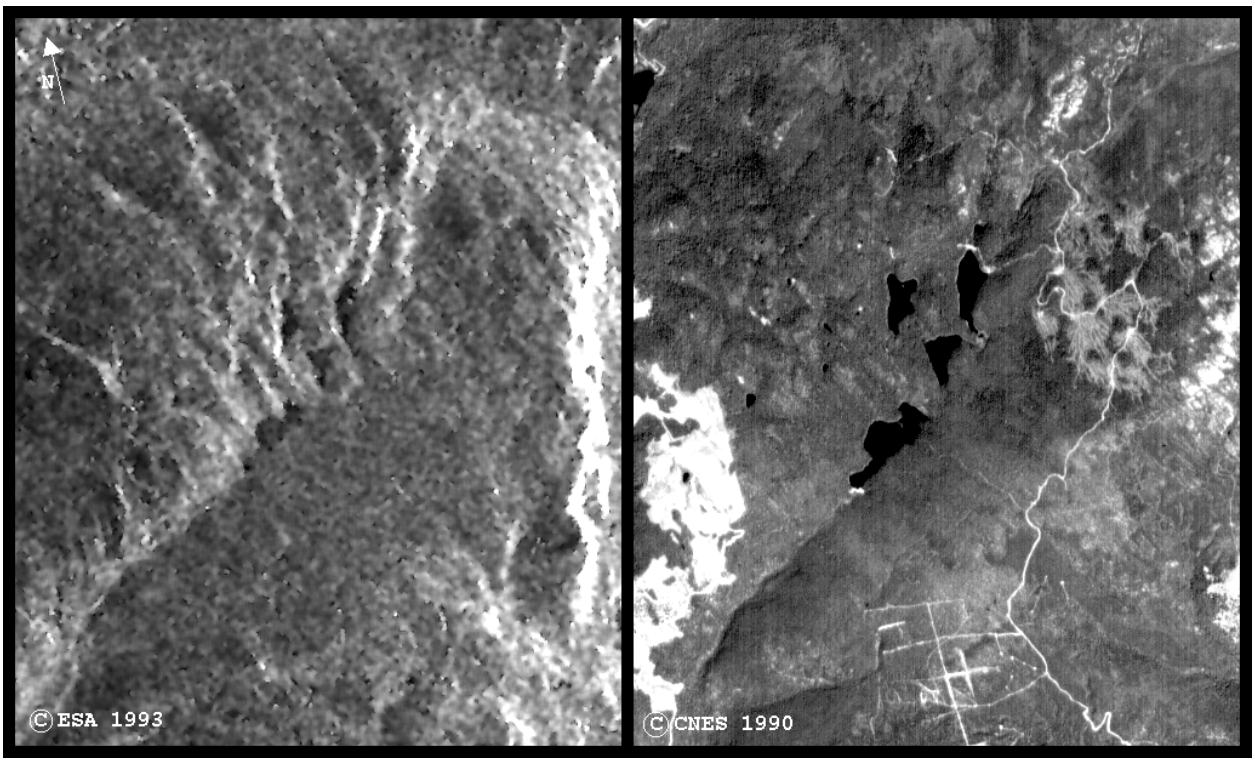

Figure 4: Moderate relief sub-area (200-m elevation and up-to-15° slopes; 500 pixels by 600 lines) of the same-side stereo pair ERS-SAR and SPOT-P10 over the Rocky Mountains, Canada. The look direction is westward oriented for the ERS-SAR ground range image (12.5-m pixel spacing) from a descending path and it is westward for the SPOT-P10 raw level 1 image (11-m pixel spacing).

2.2 Radiometric singularities

In terms of radiometry, the VIR and SAR images look very different, and can cause confusion at the beginning because interpreters prefer stereo-pairs as near identical as possible, and they are not experienced in such dissimilarity. The following radiometric singularities arise when perceiving correspondence point and depth in the combined VIR/SAR stereo-pair:

- the different response to illumination of each sensor;

- the difference in viewing angles in the azimuthal planes;
- the identification of a common spatial point or feature in the sensor output caused by the difference in terrain imaging mechanisms;
- the difference in contrast due to the dynamic range and the signal-to-noise ratio; and
- the speckle, for the SAR image, even if it is reduced with a multiple-look processing.

A mixed sensor image pair presents the greatest challenge to stereo viewing. Since depth perception is an active system, the brain can learn with training and practice to integrate the feature imaging difference and the radiometric variation caused by differences in terrain imaging mechanisms and the different responses to sensor illumination. Within this experiment, four people with different stereo-acuity practised their depth perception and stereo-fusion on this pair. Everyone obtained the general depth perception (such as in Figure 4) after different training periods (from hours to days), but only two obtained the fusion of the radiometries when features, such as roads, are quite dissimilarly imaged, such as in Figures 2 and 3. The more experienced a person is with stereoscopy, the greater their ability to perceive the depth and to fuse the different radiometries in such difficult conditions.

Another point is the difference in illumination geometry and viewing angles that generates variations in the shadow and occluded areas and their location with regard to the mountain slopes. The shadow occurs when the ground point is not illuminated by the source (backslope related to the illumination source), and the occluded area occurs when the ground point is not visible from the sensor (backslope related to the sensor). Since the illumination source is the sensor with SAR images the effects of these two concepts are mixed, but they are different with VIR images since the illumination source, the sun, and the sensor are different (mostly in "opposite" directions).

For VIR images the shadow areas are a function of the sun elevation angle. Since remote sensing VIR images are acquired during the day from the descending path of a sun-synchronous orbit, the local solar time is generally before or around noon (e.g., for SPOT, the local solar time of the descending node is 10:24 AM, Courtois et Serreault, 1980). Consequently, the sun elevation angle is high to not generate shadow even from extreme slopes, as it can be seen in Figures 2 and 3. More care should be taken with images acquired over high relief terrain in the northern or southern polar regions (more than 75° latitude) during the winter and summer seasons respectively. However this situation is not commonly encountered.

Only SAR shadow/occluded areas and VIR occluded areas are a function of the viewing angle have thus to be addressed. Since the three images were acquired from descending paths, these areas are approximately at the same location with same-side configuration, but not with the opposite-side configuration in which they are on the opposite slopes of the mountain. The situation will be inverted with ascending path SAR images. Conversely, "shadow" as a psychological cue can facilitate depth perception (mainly with our same-side stereo configuration) when combined in the brain with the binocular disparity. However, when the

slopes are smaller than 67º or 63º, there is no shadow on the ERS-SAR or occluded areas on SPOT images, respectively. Indeed figures 2 and 3 display almost no shadow/occluded areas, even in this high relief area.

A second consequence is the SAR foreshortening which occurs on only one image. Since little or no information is present in this part of the SAR image, the image content of the VIR image overcomes the brain's stereo perception. This phenomenon, as it was experienced by two of our data stereo-extraction specialists, also results in the identification of a common spatial feature (e.g., a road) that does not appear on one image. Finally, the two last points can be reduced for a better depth perception with traditional image processing techniques, such as change in image histograms, contrast stretch and speckle filtering.

In this context, since both large geometric and radiometric singularities and disparities on the stereo pair hinder stereo viewing and plotting, a reduction of one could compensate for the other. A compromise has to be reached depending on each stereo pair, the terrain and its relief. In general, it can be summarised as follows:

1) geometry: descending path images give quasi-parallel orbits and azimuthal planes, and the elevation parallax is a little reduced with opposite-side configuration;

2) radiometry: the shadow difference is minimised with same-side configuration, and shadow can be used as a psychological cue to enhance the depth perception; the dynamic range, the contrast and the speckle should be processed to minimise the differences.

Since some compromises are still conflicting, any gain achieved, for example, by a better stereo geometry could offset by any deterioration of the radiometric quality of the stereo pair. The error propagation modelling, used in accuracy assessments, has a major limitation since it is purely geometrical and neglects the thematic quality of the stereo image content (Leberl, 1990). Consequently, both opposite and same-side configurations are quantitatively evaluated in our study to address these geometric and radiometric issues.

3. STUDY SITE AND DATA SET

The study site located in British Columbia (Canada) overlaps two 1:250 000 scale maps: Hope (92H) and Penticton (82E). The area is characterised by a rugged topography where the elevation range from 400 m along Lake Okanagan to more than 2000 m on Kathleen Mountain. The land cover consists mainly of a mixture of coniferous and deciduous trees with patches of agricultural land and clear-cut areas. The agricultural fields are found mostly along Lake Okanagan, while the clear-cut areas, linked by new logging roads, are randomly located within the area. Roads are mainly loose or stabilised roads with two lanes or less, but a few are hard surface roads with two lanes or less. A few lakes and ponds are also found which are connected through a series of creeks flowing between steep cliffs. The data set consists of remote sensing data (images, orbit, attitude) and topographic data. The two SPOT images were acquired on 24 September 1989 and 11 July 1990 with a viewing angle of +26.2º (eastward looking direction, P26) and -10.4º (westward looking direction, P10) respectively. Both are raw level -1 images with ephemeris and

attitude data recorded in panchromatic mode (10-m pixel size). The ERS-1 SAR was acquired on 3 July 1993 from a descending path, with a viewing angle of -23º (westward looking direction). The image is generated in ground range projection with 12.5-m pixel spacing. The ephemeris were also recorded.

This image is a SAR standard product generally available to users. It is generated digitally during post-processing from the raw signal SAR data (Doppler frequency, time delay). Errors present in the input parameters to the image geometry model will be propagated through to the image data. These include errors in the estimation of the slant range and of the Doppler frequency, and also errors due to the satellite's ephemeris data and the ellipsoid. Assuming the presence of some geometric errors residuals, the parameters of the geometric correction model using a rigorous photogrammetric solution reflect also these residuals (Toutin, 1995a).

Two mixed-sensor stereo-pairs are then generated: an opposite-side with ERS-SAR and SPOT-P26, and a same-side with ERS-SAR and SPOT-P10. Figures 2 to 4 are sub-areas (500 pixels by 600 lines) of these two stereo-pairs. Since the three images were acquired from descending paths, geometric disparities related to the satellite and orientations of the azimuthal planes have been minimised, as mentioned earlier. But radiometric disparities related to image content are obvious: on SPOT images, the roads and the cleared areas contrast with tree and other vegetation cover. Conversely, on ERS-SAR image, when cleared areas are visible (such as the power line clear-cut) they are dark in comparison with the surrounding tree cover, whose surface roughness increases the backscatter.

The topographic data were obtained from the Canada Centre for Topographic Information, and cover an area of approximately 36 km by 28 km. The data was originally stereo-compiled from 1:50 000 scale aerial photographs taken in 1981, as observed on the surface of the Earth in cartographic X, Y and Z co-ordinates and without movement of the element due to a cartographic generalisation.

The digital cartographic data, stored in an Intergraph Graphic Design System (IGDS) file, were not clean and did not possess a topological structure. The IGDS file contained a set of planimetric entities stored in several layers. Most layers (roads, hydrography, land-covers, etc.) have a horizontal accuracy of three (3) metres, while the layer representing hydrography had a contour interval of ten (10) metres.

Areas common to the stereo-pairs and the topographic data coverage (smaller for the SAR-P26 than for the SAR-P10) were used for the evaluation of the photogrammetric stereo-restitution. It is located in the vicinity of the city of Penticton (Canada) and includes the various cartographic features discussed earlier.

4. METHODOLOGY

A pre-requisite for any stereo-mapping procedure from mixed sensors is the availability of mathematical and computer tools, which are capable of processing different image data sets. The

digital stereo workstation (DVP), used in the experiment, was first designed at the Département des sciences géodésiques et de télédétection de l'Université Laval.

The DVP, evolved as a by-product of educational tools developed at Laval University, is now a low-cost general purpose digital stereo workstation. It was first developed was to create a system on common micro-computer hardware to solve standard photogrammetric solution in a user-friendly and efficient way (Gagnon *et al.*, 1990). Subsequently, the system has been adapted at CCRS to process different airborne and spaceborne, VIR and SAR images (Toutin *et al.*, 1993; Toutin, 1995b).

The heart of the system is the mathematical modelling, which allows the combination and the simultaneous consideration of the respective image geometry to achieve optimum accuracy for the stereo-mapping process. This mathematical modelling uses the co-linearity condition as in photogrammetry, but also benefits from theoretical work in celestial mechanics to better determine the satellite orbit, and to relate the Cartesian map co-ordinates to the images co-ordinates. Further details on the geometric modelling and its applicability to visible and radar images can be found in Toutin (1995a). This modelling is used in the two main processing steps: the stereo-model set-up and the stereo-mapping.

4.1 Stereo-model set-up

To achieve high accuracy in mapping applications it is essential to determine or refine the parameters of geometric modelling using ground control points (GCPs). A bundle adjustment based on photogrammetric techniques (co-linearity and co-planarity conditions) of the two images of the stereo pair has to be performed.

Image, ephemeris and attitude (if available) data are read from the magnetic tapes and pre-processed. The SPOT images are linearly stretched over 8 bits. The SAR image is linearly compressed from 16 to 8 bits; an antenna pattern correction is applied, and a 5 x 5 gamma filter is used to reduce the speckle (Lopes *et al.*, 1993). It increases, as mentioned earlier, the quality of the stereo viewing by reducing radiometric disparities.

These data are used to initialise the different parameters of the geometric modelling. 14 GCPs (mainly road intersections) and nine (9) tie points (no ground co-ordinates) are plotted in stereoscopic mode on each stereo pair. The accuracy of the image co-ordinates is about one pixel (10-12 m). The ground co-ordinates of the GCPs were previously acquired on a traditional stereo plotter using the aerial photographs at CCTI. The accuracy of the cartographic co-ordinates is in the order of 3 m. The tie points are useful to reinforce the stereo geometry and fill in gaps in the stereo model, where there are no GCPs, because they contribute additional conditions to the equations system. Results for each stereo pair of the iterative least square bundle adjustment are presented in Table 1 (root mean square, RMS, minimum and maximum residuals). Previous studies (Toutin, 1995a) have shown that this geometric modelling is not affected by the number, the density and the spatial distribution of the GCPs because it respects the global viewing geometry (sensor + platform + Earth), if there is no extrapolation in planimetry and in altimetry.

Table 1: Results (in metres) on the bundle adjustment for each stereo pair with the root mean square (RMS), minimum and maximum residuals on the 14 GCPs.

Stereo-pair	**Opposite-side SAR - P26**			**Same-side SAR - P10**		
Residuals	X	Y	Z	X	Y	Z
RMS	13.3	15.0	11.0	14.8	14.9	13.4
Minimum	-27.6	-30.2	-20.2	-27.4	-33.5	-20.1
Maximum	+16.5	+37.5	+16.8	+18.8	+28.8	+30.8

The RMS residuals which are in the same order of magnitude of the GCP plotting error and which represent an a-priori stereo-mapping error are then a good indication of the final results. As a consequence, the stereo model is generated directly from the raw images (without any resampling) with a y-parallax of around one pixel. The y-parallax between the two images of a stereo-pair is automatically cancelled at the floating marks when the operator moves in the stereo model. When the operator cancels the x-parallax to fuse the two floating marks at the measured point, a least square stereo intersection is performed in real time using the previously computed geometric modelling to convert the images co-ordinates to the cartographic co-ordinates (X, Y, Z) of the user defined map projection system.

Although the same-side stereo pair displays a larger elevation parallax (Figure 1), there is no significant difference in the result for the two stereo pair configurations. Errors in the plotting should have generated more errors in the opposite-side stereo pair due to the weaker geometry intersection. This has to be confirmed with the larger checked data sampling during the stereo-mapping step.

4.2 Stereo-mapping

Stereo-mapping does not only imply DEM generation, but also planimetric feature extraction, which so far has been one of the most neglected issues (Grün, 1997). As mentioned by Raggam *et al.* (1994), automatic procedures may cause problems due to the radiometric differences of the images and may generate errors larger than the stereoscopic process by itself, and then hinder accuracy evaluation. Consequently, measurements for corresponding image points were done interactively by a human operator using the DVP stereoscopic apparatus to determine the best achievable accuracy. But in an operational environment a hybrid approach, which combines human depth perception and semi-automatic measurement by the computer should be considered.

For planimetry, roads, railroads, power lines, and lakes are extracted. Depending on the thematic applications, other planimetric features could be extracted taking into account the radiometry of both sensors. For the altimetry, the height measurements are extracted on a ten pixel regular grid on the left image, this generates an irregular grid of points when projected to the ground system.

5. RESULTS AND ANALYSIS

Depending on the feature and the stereo-pair, different amounts of data are extracted. First, the data are imported in a geographic information systems (GIS) environment to be compared with the topographic data. Next, "buffered" zones, centred on the topographic feature, are generated at 6, 12, 20, 30, 40, and 50 m. These buffered zones act as corridors "parallel" to the topographic feature at difference distances and they are used for the comparison of the stereo extracted features with the map features. Therefore, it is possible to quantify the cumulative distance of stereo-extracted features within each zone. The percentage (ratio between the distance of the zone and the total distance) for each zone and the cumulative percentage of linear distance can then be computed. For example, Table 2 gives the full results of the stereo-pairs for the roads, and Table 3 gives the result summary for all features. It includes the cumulative distance of extracted data, the root mean square (RMS) error at 66% confidence and the 90% confidence error.

Table 2: Results of the comparison for roads extracted from SAR-P26 and SAR-P10 stereo-pairs and the checked topographic data.

Accuracy (metres)	**Opposite-side SAR-P26**			**Same-side SAR-P10**		
	Distance (metres)	Percentage (%)	Cumulative Percentage	Distances (metres)	Percentage (%)	Cumulative Percentage
6	9195.0	11.0	11.0	13829.9	12.2	12.2
12	11022.4	11.9	22.9	14185.7	12.6	24.8
20	14201.1	15.3	38.2	19652.8	17.4	42.2
30	19977.6	21.5	59.7	28526.5	25.3	67.5
40	18681.0	20.1	79.8	22755.4	20.2	87.7
50	11526.3	12.4	92.2	8889.6	7.9	95.6
50+	7531.8	8.1	97.7	4921.4	4.4	100.0
Total	93098.1		100.0	112761.2		100.0

5.1 Roads accuracy assessment

Since the aerial photographs and the satellite data were taken 8 to 10 years apart, and the area has intensive forest activity, the new logging roads were not extracted or used in the evaluation. Tables 2 and 3 show 32-m and 29-m RMS errors (66%) and 48-m and 42-m error with 90% confidence for the opposite-side SAR-P26 and same-side SAR-P10 stereo-pairs, respectively. Each linear entity that had an error greater than the 90% confidence error was visually compared by importing the topographic file into the DVP. The origins of most of these errors were due to physical changes in position between 1981 and 1990, to the interpretation variation in locating curves and intersections, and to the definition of logging roads in their context. Results are less promising for the SAR-P26 stereo-pair mainly due to the poorer radiometric contrast of the SPOT-P26 image (Figure 2 when compared with Figure 3).

Table 3: Results summary (RMS and 90% confidence errors in metres) of the comparison for all features extracted from SAR-P26 and SAR-P10 stereo pairs and the checked topographic data.

Stereo-pair	**Opposite-side SAR-P26**			**Same-side SAR-P10**		
Planimetric Feature	Cumulative Distance	66% Confidence RMS Error	90% Confidence Error	Cumulative Distant	66% Confidence RMS Error	90% Confidence Error
Roads	93098	32	48	112761	29	42
Railroads	6171	41	52	6181	27	38
Power Lines	10983	35	49	20720	29	48
Lakes	12623	25	46	13791	30	46

5.2 Railroads accuracy assessment

Table 3 shows 41-m and 27-m RMS errors and 52-m and 38-m errors with 90% confidence for the SAR-P26 and SAR-P10 stereo pairs, respectively. Although the railroad information is present sometimes in the ERS SAR, the difficulty of identifying the railroads located along a cliff (shaded area) or close to a road on the SPOT image explains the larger error in the SAR-P26. The better contrast and radiometry range of the P10 image explains the better results for this SAR-P10 stereo pair. This variation can be noted with Figures 2 and 3 at the bottom of the main valley.

5.3 Power lines accuracy assessment

Table 3 shows 35-m and 29-m RMS errors and 49-m and 48-m errors with 90% confidence for the SAR-P26 and SAR-P10 stereo-pairs, respectively. The larger errors are mainly due to the fact that power lines are not visible on the satellite images, but are extracted as being the middle of the clear-cut, which is not always the physical reality. Furthermore, the extraction of this feature out of the forest is more difficult due to less contrast with the surroundings.

5.4 Lake accuracy assessment

Table 3 shows 25-m and 30-m RMS errors and 46-m and 46-m errors with 90% confidence for the SAR-P26 and SAR-P10 stereo-pairs, respectively. The larger errors are due to the variation in the shape of the lake, not only between the two images but mainly with the topographic file. They “shrank” during the summer and the fall. On the satellite stereo-pairs the lakes were determined by the current shoreline, because the “high water limit” (used for the aerial photos) was not visible. Acquisition dates could be a key factor for extracting this feature.

These general results show that accuracy as a function of the stereo-pairs has no special trend. The accuracy of the planimetric features is not correlated to the stereo configuration, opposite or

same-side. It is also consistent with the results of the a-priori stereo-mapping (Table 1) the stereo-plotting process. Since the operator always plots at the vertical of the point to be extracted, an error in elevation has no impact on the planimetric accuracy. In other words, a stronger stereo geometry such as the same-side SAR-P10 stereo-pair (Figure 1) does not provide better results for the planimetric feature extraction.

This confirms previous studies (Toutin, 1997), that show that planimetric accuracy is –except for the extreme case- independent of the intersection angle, but mainly dependent on the radiometry. This dependency on radiometry explains the variations in the results for the different stereo-pairs and planimetric features:

- the image content which is related to the specificities of the sensor (SAR versus VIR; active versus passive, resolution);

- the general dynamic range of each sensor and the contrast in each image;

- the definition and the physical characteristics of each feature, such as difficulty in locating intersection and small curves for the logging roads, the positioning of the power line inside the clear-cut, the "true" lake shoreline, etc.; and

- the contrast of each feature within its surrounding such as road in bare soil or in forest, lake very separable from forest unless wind induced surface roughness increases the backscatter, power line outside of the forest.

In general, the image contents of the SPOT-P image "provides" the information on the feature, while the ERS-SAR combined with SPOT-P provides the third dimension with the stereo viewing. Indeed, when the feature is also visible on the SAR image (power line clear-cut, lake), it does not necessarily imply a better result. It seems that the brain prefers the image where the "best planimetric" feature occurs. A better understanding of different depth perception mechanisms by the brain should help to understand the phenomenon of stereoscopic viewing with this kind of challenging data.

5.5 Elevation accuracy assessment

For the height measurement a first evaluation was performed to quantify the relative pointing error in elevation. Twenty points, which span different features and cover features such as woods, rock, clear-cut area, roads, or cliffs etc., were chosen. It should be noted that these are not necessarily identifiable features. By stereo-pointing these points five times will lead to a ±3 m and ±5 m elevation pointing precision for SAR-P26 and SAR-10 stereo-pairs, respectively. Furthermore, 20 clearly identifiable check points with known ground co-ordinates (accuracy better than 5 m) were plotted on the stereo model three times each to quantify the absolute elevation accuracy at spot elevation points. RMS elevation errors of 12 m and 15 m were obtained for SAR-P26 and SAR-P10 stereo pairs, respectively.

About 3900 and 4200 points (irregular DEM) are acquired on the SAR-P26 and SAR-P10 stereo pairs, respectively and directly compared to a fine grid spacing DEM generated from the 10 m contour lines with the GIS functions. This avoids errors generated by any processing to transform this irregular DEM into a regular grid, since the objective was to assess the accuracy of the extracted data and not to generate a regular DEM. Table 4, Figures 5 and 6 give the statistics generated from the comparison for SAR-P26 and SAR-P10 stereo-pairs respectively.

Table 4: Statistical results (in metres) generated from the comparison of the stereo extracted DEMs and the fine grid spacing DEM generated from the 10 m contour lines of the 1:50 000 topographic data

Stereo-pair	**Opposite-side**	**Same-side**
Errors (m)	**SAR-P26**	**SAR-P10**
Bias	+0.5	-3
RMS	19	20
Minimum	-84	-84
Maximum	+141	+94

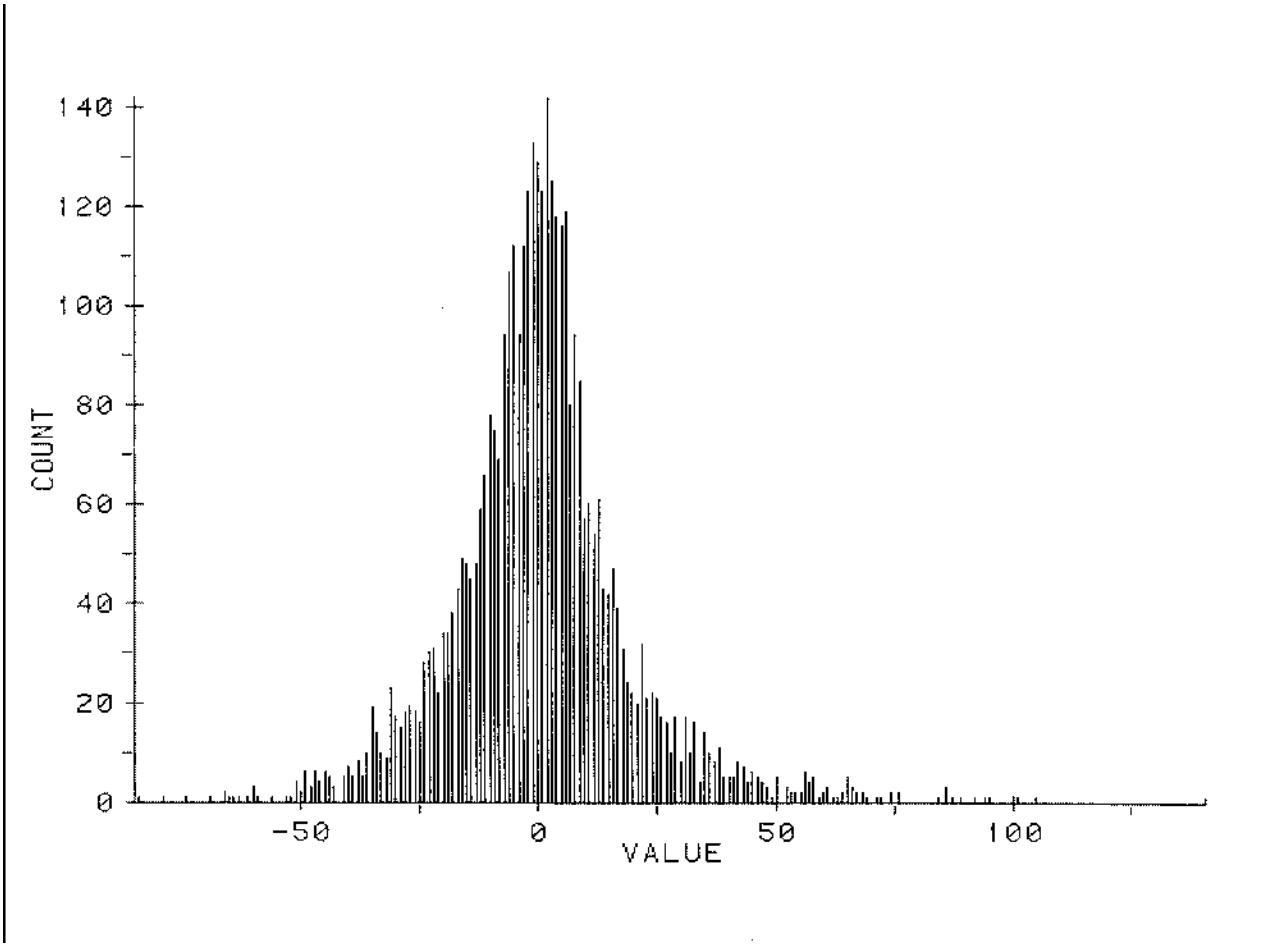

Figure 5: Statistics generated from the comparison of the DEM stereo extracted from the opposite-side SAR-P26 stereo-pair with the 10-m contour topographic derived DEM.

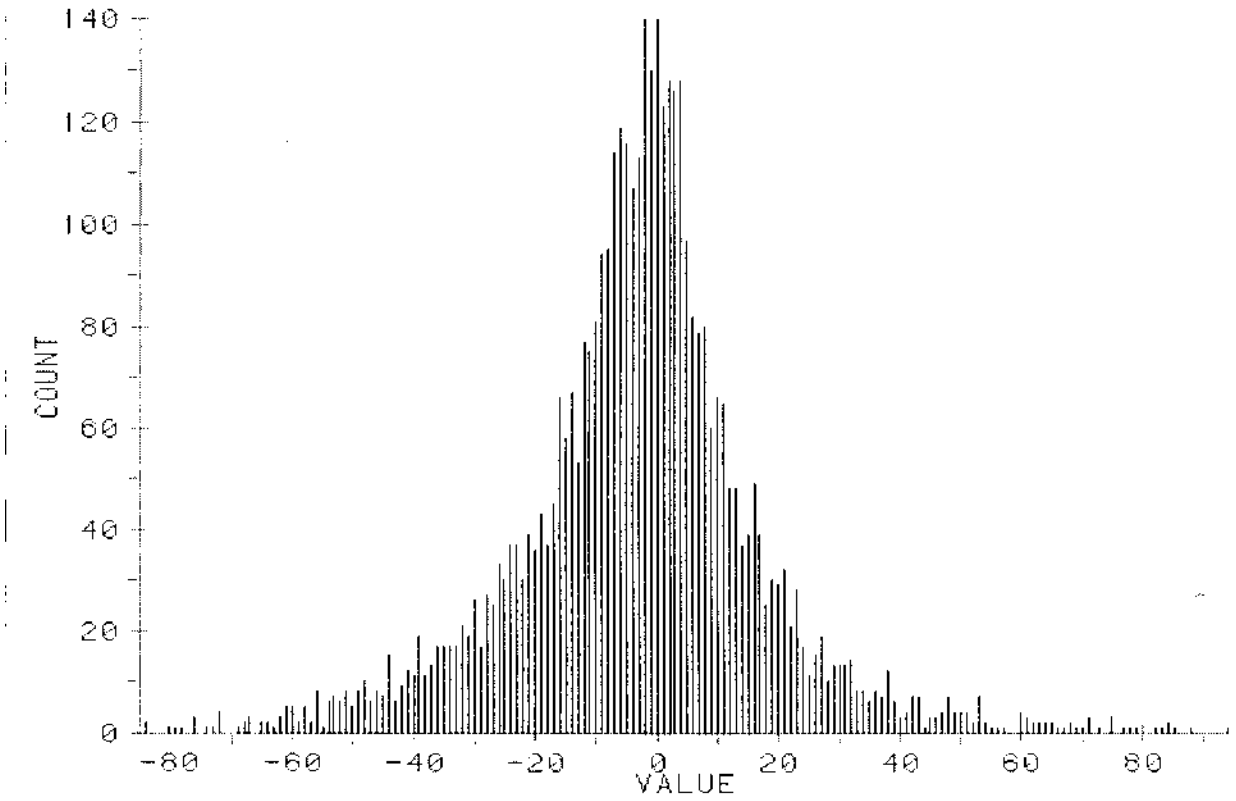

Figure 6: Statistics generated from the comparison of the DEM stereo extracted from the same-side SAR-P10 stereo-pair with the 10-m contour line topographic derived DEM.

Compared to the spot elevation accuracies computed previously, the 19-m and 20-m RMS errors for the SAR-P26 and SAR-P10 stereo pairs, respectively, are consistent. The difference is due to the fact that DEM points are rarely well-identifiable points unlike the spot elevation points. Furthermore, an identifiable feature also helps the brain to fix the stereo model into the space, especially with this mixed sensor data set.

We can note that Figures 5 and 6 and Table 4 do not strongly support the expectation that larger intersection angles or parallaxes translate into higher elevation accuracy since the difference between the two RMS errors is only one metre and the histograms are quite similar (bias, minimum and maximum). Previous results involving stereo SAR data, mainly with SIR-B, do not concur with the theory (Leberl, 1990), especially in high relief terrain.

The only parameter studies evaluated for accuracy addressed theoretical error propagation (Leberl, 1990). The major limitation of error propagation modelling is the fact that it is purely geometrical and neglects the thematic image quality of the stereo-pairs, but also some other non-quantitative and psychological cues related to human depth perception. When only SAR images

are involved in the stereo-pair, it is understandable that as the viewing angles differ more, the quality of the stereo fusion, deteriorates thereby setting off any gain achieved by a better stereo geometry, as mentioned in a previous section.

But in our experiment, since the same SAR image and "almost two radiometrically similar" SPOT-P images (except for the contrast) are used in the two stereo-pairs, the radiometric aspects should not be the reason to set off the stronger geometry of the SAR-P10 stereo-pair. But, as discussed in a previous section with Figure 1, the SPOT-P contribution to the elevation parallax is very small when compared to the ERS-SAR contribution for both stereo configurations (about 10-20%). Consequently, the difference between the elevation parallaxes of the two stereo-pairs is not very large. They thus have a "equivalent" stereo geometry. However, the largest parallax could make the stereo viewing more difficult, and could destroy the strongest geometry.

Table 4 also shows that some of the errors are large, about 60-70 points for each stereo-pair, and are over three times the RMS error. By selecting and displaying these points on the DVP, it may be seen that they are spatially grouped rather than randomly distributed and they are not the same between the two stereo-pairs. These points are located at different ranges and different topography in the stereo model. But, most of them (about 40) are located in the strongest slopes, where foreshortening and shadow occur in the ERS-SAR image. Since the stereo viewing is local in this area, the operator can sometimes loose the stereo viewing with extreme parallax or when the two floating marks are too far from the "good" position. The operator's fatigue also affects the propagation and increase of errors under these specific conditions. As a matter of fact, re-plotting these points more carefully reduces their error inside three times the RMS error. The brain also has more time during the re-plotting "to interpret" the two images in this difficult situation.

6. CONCLUSIONS

Geometric and radiometric disparities between SAR and VIR images can hinder stereoscopic viewing. Since depth perception is an active and sophisticated process involving eye vision and brain activities to perceive and understand depth, a human operator can learn and acquire this "non-natural" stereo capability with time and practice. The more experienced with stereo viewing the operator is, the faster and better are the training and the results, as was demonstrated by our operators. But compromises have to be made to minimise the geometric and/or radiometric disparities, such as acquiring images from descending path to give quasi-parallel satellite tracks and azimuthal planes, reducing the elevation parallax, processing the radiometry (dynamic range, contrast, speckle). These facilitate stereo viewing and plotting from a mixed sensor stereo-pair.

This paper then presented quantitative results of data extraction in planimetry and altimetry from challenging mixed-sensor ERS-SAR and SPOT-P stereo-pairs on a PC-based stereo workstation using photogrammetric techniques. The first stereo-pair, SAR-P26, is an opposite-side viewing, which generates a destructive elevation parallax, and the second one, SAR-P10, is a same-side viewing, which generates a constructive elevation parallax. The mathematical equations, which

drive the DVP, are based on the co-linearity and co-planarity conditions. They represent the physical reality of the full geometry of viewing: platform, sensor and Earth.

From the raw images, the data are interactively stereo-extracted and transferred to a GIS environment. Compared to accurate digital topographic data, planimetric and altimetric accuracies have been computed for different features (roads, railroads, power lines, lakes, spot elevation points and DEM).

In planimetry, the accuracies for the opposite-side stereo-pairs are 32 m, 41 m, 35 m and 25 m for the roads, railroads, power lines and lakes, respectively. For the same-side stereo-pair, they are 29 m, 27 m, 29 m and 30 m for the roads, railroads, power lines and lakes, respectively. The difference in the results between the stereo-pairs is due to the definition of each planimetric feature and the radiometric quality of each SPOT image. The geometry does not affect the accuracies, since the operator extracts along the vertical axis. In altimetry, 12 m and 15 m accuracies for spot elevation points and 19 m and 20 m accuracies for the DEM have been computed with the opposite-side and same-side stereo-pairs, respectively. There was no significant bias. Larger errors occurred mainly in the strongest slopes where foreshortening and layover arise in ERS-SAR images. In these areas, local stereo viewing can be lost due to extreme parallaxes, when the floating marks are too far from the "good solution". Re-plotting more carefully reduces the error in these areas. Location on the stereo-model does not affect these accuracies.

The stronger geometry with the same-side SAR-P10 images does not achieve significant improvement in the elevation accuracies, contrary to theoretical expectations. Since there are few differences in radiometry between the two stereo-pairs, it cannot offset any gain achieved by a better stereo-geometry. One potential reason is that the elevation parallax in both stereo-pairs is mainly dominated by the SAR geometry.

We can summarise the results of the stereo- restitution from a mixed-sensor stereo-pair:

1. the radiometry of the SPOT-P images mainly contribute to the determination of the planimetric feature with the quality of its image content; and
2. the geometry of the ERS-SAR image mainly contributes to the determination of the elevation with its high sensitivity to the terrain relief.

ACKNOWLEDGMENTS

The author would like to thank his CCRS colleagues as well as the anonymous external reviewers for their critical review to improve this paper. He would also like to thank Liyuan Wu of Consultants TGIS inc. for the data stereo extraction in the challenging stereo-pairs.

REFERENCES

M. Courtois et B. Serreault*, Acquisition et choix de l'orbite SPOT", Le mouvement du véhicule spatial en orbite*, (Toulouse, France: CNES), pp.659-702, 1980.

R. Friedhoff and W. Benzon, *The Second Computer Revolution: Visualization*, (New York: W.H. Freeman and Company), 1991.

P.A. Gagnon, J.P. Agnard, C. Nolette, and M. Boulianne, "A Micro Computer-based General Photogrammetric System", *Photogrammetric Engineering and Remote Sensing*, vol. 56, no. 5, pp. 623-625, 1990.

A. Grün, "Digital Photogrammetric Stations: A Short Best of Unmatched Expectations", *Geo Info Magazine*, Vol. 11, no. 1, pp. 20-23, 1997.

B. Guindon and M. Adair, "Analytic Formulation of Spaceborne SAR Image Geocoding and Value-Added Product Generation Procedure using Digital Elevation Data", *Canadian Journal of Remote Sensing*, Vol. 18, no. 7, pp. 2-12, 1992.

C. Heipke, "State-of-the-Art Digital Photogrammetric Workstations for Topographic Applications", *Photogrammetric Engineering and Remote Sensing*, vol. 61, no. 1, pp. 49-56, 1995.

R.R Hoffman, "Remote Perceiving: A Step Toward a Unified Science of Remote Sensing", *Geocarto International*, vol. 5, no. 2, pp. 3-13, 1990.

F. Leberl, *Radargrammetric Image Processing*, (Norwood, MA: Artech House), 1990.

A. Lopes, E. Nezry, R. Touzi and H. Laur, "Structure Detection and Statistical Adaptive Speckle Filtering in SAR Images", *International Journal of Remote Sensing*, Vol. 14, no. 9, pp. 1735-1758, 1993.

T. Okoshi, *Three-Dimensional Imaging Techniques*, (New York: Academic Press), 403p., 1976.

H. Raggam, A. Almer, and D. Strobl, "A combination of SAR and Optical Line Scanner Imager for Stereoscopic Extraction of 3D Data", *ISPRS Journal of Photogrammetry and Remote Sensing*, vol. 49, no. 4, pp. 11-21, 1994.

Th. Toutin, C. Nolette, Y. Carbonneau, and P.A. Gagnon, "Stéréo restitution interactive des données SPOT: description d'un nouveau système", *Journal canadien de télédétection*, vol. 19, no. 2, pp. 146-151, 1993.

Th. Toutin, "Multi-source data fusion with an integrated and unified geometric modeling", *EARSeL Journal, "Advances in Remote Sensing"*, vol. 4, no. 2, pp. 118-129, 1995a.

Th. Toutin, “Generating DEM from Stereo-Images with a Photogrammetric Approach”, *EARSeL Journal, “Advances in Remote Sensing”*, vol. 4, no. 2, pp. 110-117, 1995b.

Th. Toutin, “Accuracy Assessment of Stereo-Extracted Data from Airborne SAR Images”, *International Journal of Remote Sensing*, vol. 18, no. 18, pp. 3693-3707, 1997.

I.V. Yelizavetin, “Digital Terrain Modeling from Radar Image Stereo-Pairs,” *Mapping Sciences and Remote Sensing*, vol. 30, no. 2, pp. 151-160, 1993.